

BIOCOMPATIBLE AND ANTIMICROBIAL CELLULOSE ACETATE  
 NANOFIBER MEMBRANE FROM BANANA (*MUSA ACUMINATA X  
 BALBISIANA*) PSEUDOSTEM FIBERS FOR WOUND HEALING  
 AND TISSUE ENGINEERING

CARLO M. MACASPAG, JENNELI E. CAYA and JULIUS L. LEAÑO JR.

*Natural Fiber Utilization Section, Research and Development Division, Philippine Textile Research  
 Institute, Department of Science and Technology, Bicutan, Taguig City, 1630, Philippines*

✉ *Corresponding author: C. M. Macaspag, cmmacaspag@gmail.com*

*Received January 25, 2023*

Electrospun nanofiber membranes play a vital role in the biomedical field, especially for wound healing and tissue engineering applications. This study explored the development of biocompatible and antibacterial cellulose acetate electrospun nanofiber membranes prepared from banana pseudostem fibers. Cellulose rich dissolving pulp from alkali treated banana pseudostem fibers was subjected to esterification reaction to produce cellulose acetate. The synthesized cellulose acetate and chlorhexidine (CHX), an antimicrobial agent, were dissolved in 2:1 acetone:*N,N*-dimethylacetamide solvent and subsequently electrospun into a nanofiber membrane. FT-IR spectroscopy of the nanofiber confirmed the presence of cellulose acetate and the successful incorporation of CHX into the nanofibers. SEM imaging showed that the fiber diameter of the nanofiber membrane ranged from 200 nm to 300 nm. The MTT cytotoxicity assay and antimicrobial assay of nanofibers revealed that the nanofiber membrane with chlorhexidine concentration of 1.0 w/v was the optimum formulation as it achieved potent antimicrobial activity (zone of inhibition (ZOI): *Escherichia coli* – 18.38 mm and *Staphylococcus aureus* – 22.51 mm), while exhibiting low cytotoxicity to human intestinal epithelial cell line, HIEC-6 (percent cell inhibition: 13.07% and IC<sub>50</sub>: >100 µg/mL). The results indicated successful preparation of biocompatible and antimicrobial nanofiber membranes from banana pseudostem fiber with potential application in wound healing and tissue engineering.

**Keywords:** biocompatible, antimicrobial, cellulose acetate, nanofibers

## INTRODUCTION

Biomaterials used for wound healing are prepared in different physical forms: as nanofibers,<sup>1</sup> films,<sup>2</sup> hydrogels<sup>3</sup> and porous spongy matrices.<sup>4</sup> Among these forms, nanofibers present a number of advantages: they can absorb excess exudate, mimic the extracellular matrix during the proliferation stage of wound healing, facilitate efficient exchange of oxygen and nutrients within the wound area and support the adhesion and proliferation of cells, which hastens the formation of collagen during the wound healing process.<sup>5</sup>

Cellulose acetate is considered an ideal scaffold material for wound healing and tissue engineering applications, due to its good mechanical properties and ease of processability.<sup>6</sup> Also, cellulose acetate renders excellent biocompatibility and biodegradability, which is

beneficial for wound healing and tissue engineering.<sup>7</sup>

Cellulose acetate (CA) is a man-made polymer obtained through esterification of cellulose by acetic acid and acetic anhydride, resulting in the substitution of an acetyl group for some of the hydroxyl groups of cellulose. Amongst the derivatives of cellulose, CA has drawn a great deal of attention due to its processability in comparison with cellulose. CA is known for its properties that make it most suitable for biomedical engineering – biodegradability, biocompatibility, insolubility in water, mechanical properties, nontoxicity, high affinity, good hydrolytic stability, relatively low cost and excellent chemical resistance. CA can be potentially utilized for wound dressings, as well

as other potential applications as antimicrobial membranes, filament-forming matrix, biomedical nanocomposites, affinity membranes and biomedical separation.<sup>8</sup>

Recent studies conducted on CA have focused on its conversion into nonwoven membranes via electrospinning, which involves the dissolution of CA in an appropriate solvent. The solubility of CA depends on the degree of the substitution of the acetate group. The most suitable solvents to prepare CA nanofibers are acetone, methanol, chloroform, dimethylacetamide, dimethylformamide, formic acid, trifluoroacetic acid, acetic acid or a blend of these.<sup>9-12</sup> Moreover, compared to natural cellulose, CA can be more easily electrospun into nanoscale membranes, films and fibers.<sup>13</sup>

Banana (*Musa* sp.) is widely cultivated in tropical and subtropical countries. It is a perennial, single-harvest plant grown primarily for its fruit. After the fruit harvest, the whole plant is decapitated to allow young suckers to replace the mother plant.<sup>14</sup> This cycle can continue for several generations before banana fruit production significantly declines. Generally, banana by-products include the pseudostem, leaves, inflorescence, fruit stalk, rhizome and peels.<sup>15</sup> The stem is a significant by-product, produced in amounts of about 100 metric tons per hectare annually. In practice, the banana pseudostem is left to rot on the soil to replenish the nutrients for growth of the next banana generation. However, this treatment represents a huge loss of biomass and generates a large amount of carbon dioxide, as well as unpleasant odor, presenting a serious environmental concern.<sup>14,15</sup> This type of management can also induce the growth of banana fusarium wilt caused by *Fusarium oxysporum* f. sp. *cubense*, which is one of the most serious fungal diseases in bananas and a major limiting factor in worldwide banana production.<sup>16</sup> These considerations have led to a number of researches geared towards the utilization of banana pseudostem for a variety of uses, including textiles, fiber reinforced composites, biogas production, enzyme production, pulp and paper manufacturing.<sup>17</sup>

Previous studies have focused on the preparation and subsequent characterization of cellulose nanofibers from agricultural by-products,<sup>18-21</sup> but few efforts are known to the authors on using such residues for the preparation of biocompatible and antimicrobial cellulose-based nanofiber membranes. This study aims to

valorise agricultural by-products, such as the banana pseudostem fibers, by producing high cellulose content dissolving pulp, for further development of biocompatible and antimicrobial cellulose acetate nanofiber membranes intended for biomedical applications. This valorization of agricultural by-products would pave the way for the production of functional biomaterials for healthcare applications with environmental benefits.

## EXPERIMENTAL

### Materials and reagents

Banana (*Musa acuminata* x *balbisiana*) pseudostems were sourced from a local banana cultivator. Glacial acetic acid (CH<sub>3</sub>COOH, 99%, JT Baker), acetic anhydride ((CH<sub>3</sub>CO)<sub>2</sub>O, 98%, JT Baker), sulfuric acid (H<sub>2</sub>SO<sub>4</sub>, 98%, JT Baker), ethanol (CH<sub>3</sub>CH<sub>2</sub>OH, 99.5%, RCI Labscan), hydrochloric acid (HCl, 37%, RCI Labscan), sodium hydroxide (NaOH, 98%, Loba Chemie), *N,N*-dimethylacetamide (99.5%, Loba Chemie), acetone ((CH<sub>3</sub>)<sub>2</sub>CO, 99.5%, RCI Labscan), sodium metabisulfite (Na<sub>2</sub>S<sub>2</sub>O<sub>5</sub>, 97%, JT Baker) and phenolphthalein (indicator grade, Loba Chemie) were all of analytical grade and used without further purification. Sodium silicate and hydrogen peroxide were technical grade chemicals and sourced from local suppliers.

### Fiber treatment

Banana fibers were subjected to alkaline treatment prior to the synthesis of cellulose acetate. The fibers were treated in a boiling solution (liquor ratio of 1:15) containing 12% NaOH, 1.0% sodium metabisulfite and 0.05% anionic liquid detergent for 2 h. Then, the fibers were rinsed with hot water to remove the residual chemicals. The degummed fibers were subjected to scouring and bleaching by immersing the fibers into a boiling solution (liquor ratio of 1:15) containing 4 g/L NaOH, 2 g/L sodium silicate, 8 g/L hydrogen peroxide and 0.5 g/L detergent for 30 min. The fibers were then washed with hot water thrice and neutralized with 1% acetic acid. The degumming, scouring and bleaching were repeated with reduced NaOH concentration to 6% for degumming, while the concentration of chemicals and conditions of the process remained the same. The fibers were finally washed with distilled water and air dried for 24 h.

### Synthesis of cellulose acetate

Banana fibers were converted into cellulose acetate through esterification and partial saponification reactions. The treated banana fibers were first powdered using a Wiley Mill with a 60 mesh screen filter. 10 g of the fibers were reacted with 50 mL of glacial acetic acid in the presence of 0.5 M concentrated sulfuric acid. The reaction mixture was left to stand for 1 h at room temperature. Then, 50 mL

of acetic anhydride and 20 mL of glacial acetic acid were added to the reaction mixture. The mixture was placed in a water bath at 50 °C for 30 min. After that, 50 mL of 70% acetic acid and 0.14 mL of sulfuric acid were slowly added to the reaction mixture at constant temperature of 80 °C for 3 h. The product was precipitated from the reaction mixture using deionized water. The cellulose acetate precipitate was filtered using a vacuum filtration set-up and the product was washed with deionized water until the pH of the filtrate was neutral. The product was dried in a vacuum oven at 60 °C and 500 millibar.

#### Drug loading and electrospinning of cellulose acetate nanofiber membrane

40% w/v cellulose acetate polymer solution was prepared from 2:1 acetone:*N,N*-dimethylacetamide binary solvent. The polymer solutions were then loaded with different concentrations of antimicrobial drug chlorhexidine (CHX) (0.0% w/v, 0.5% w/v, 1.0% w/v and 1.5% w/v) and were subjected to electrospinning to produce nanofiber membranes.

The electrospinning run was performed using the following parameters: voltage: 12 kV, tip to collector distance: 15 cm, flow rate: 1.0 mL/h.

#### Fiber analysis

Raw and alkaline treated banana fiber were subjected to various fiber analyses prior to the synthesis of cellulose acetate: moisture content (PTRI Standard Method No. 37-1974), alcohol benzene extractives (TAPPI T204 cm-97), lignin content determination (TAPPI T222 om-98), total cellulose and alpha cellulose (TAPPI T203).

#### Degree of substitution determination

The degree of substitution (DS) of the synthesized cellulose acetate was determined by the titration method. 20 mL of ethanol was added to 0.5 g of synthesized cellulose acetate and reagent blank. 0.5 N NaOH was added to the solutions and heated for 15 min. The solutions were then kept for 72 h under ambient conditions. The excess alkali was then titrated with 0.5 N HCl using phenolphthalein indicator. After titrating the excess alkali, an excess 1 mL of 0.5 N HCl was added and then back titrated with 0.5 N NaOH. The DS of the synthesized cellulose acetate was calculated using the formula:

$$\% \text{ acetyl} = \frac{[(A-B) N_b - (C-D) N_a]}{W} \times 4.3 \quad (1)$$

$$DS = \frac{(3.86 \times \% \text{ acetyl})}{(102.4 - \% \text{ acetyl})} \quad (2)$$

where: A is the amount of NaOH (in mL) added to the sample, B is the amount of NaOH (in mL) added to the blank, C is the amount of HCl (in mL) added to the sample, D is the amount of HCl (in mL) added to the blank,  $N_b$  is the normality of the NaOH solution,  $N_a$  is the normality of the HCl solution, W is the weight of the sample.

#### Fourier transform-infrared spectroscopy (FT-IR)

FT-IR spectra of the cellulose acetate powder, electrospun cellulose acetate nanofiber (CANF) and electrospun CHX loaded cellulose acetate nanofiber (CHX-CANF) were recorded at room temperature in the mid-IR range (400  $\text{cm}^{-1}$  – 4000  $\text{cm}^{-1}$ ) on a Bruker Tensor 27 FT-IR spectrometer, equipped with a Bruker Platinum ATR accessory, with a single reflection diamond crystal. Each spectrum was averaged over 128 scans with a resolution of 2  $\text{cm}^{-1}$ . A background scan was recorded prior to the measurement and subtracted from the sample spectra.

#### Scanning electron microscopy-energy dispersive X-ray spectroscopy (SEM-EDX)

Electrospun cellulose acetate nanofiber (CANF) and electrospun CHX loaded cellulose acetate nanofiber (CHX-CANF) were analyzed using a Dual Beam Helios Nanolab 600i. The SEM was operated at accelerating voltage of 5.0 kV and beam current of 0.17 nA, while the EDX was operated at accelerating voltage of 10.0 kV and 0.69 nA. SEM images were acquired from 100x to 20,000x magnification. The fiber diameter of the nanofiber membranes was measured using the ImageJ software. The acquired EDX spectra of the electrospun nanofiber and drug loaded nanofiber membrane were used to determine the weight percentage of the elements present in the nanofiber membrane.

#### Biocompatibility of nanofiber membrane

Electrospun cellulose acetate nanofiber (CANF) and electrospun CHX loaded cellulose acetate nanofiber (CHX-CANF) were subjected to the MTT cytotoxicity assay using a human intestinal cell line (HIEC-6) to assess cell viability. For this assay, HIEC-6 cells were seeded at  $6 \times 10^4$  cells/mL in the sterile 96-well plate of the UV-Vis spectrophotometer. Eight two-fold dilutions of CANF and CHX-CANF samples were used as treatments starting from 100  $\mu\text{g/mL}$  down to 0.78  $\mu\text{g/mL}$ . Mitomycin C served as positive control, while dimethyl sulfoxide (DMSO) served as negative control. Following incubation, the HIEC-6 cells were treated with each CANF and CHX-CANF dilutions. The treated cells were again incubated for 72 hours at 37 °C and 5%  $\text{CO}_2$ . Following the incubation, CANF and CHX-CANF dilution solutions were removed and 3-(4,5-dimethylethylthiazol-2-yl)-2,5-diphenyltetrazolium bromide (MTT) dye at 0.5 mg/mL PBS was added. The cells were again incubated at 37 °C and 5%  $\text{CO}_2$  for 4 hours. DMSO was then used to dissolve the formazan crystals formed by the reduction of the dye by the live cells. Absorbance measurement was done at 570 nm. The GraphPad Prism 6 software was used to compute for the Inhibition Concentration 50 ( $\text{IC}_{50}$ ) of the sample by employing the non-linear regression curve fit on the computed percent inhibition per concentration of the sample.<sup>22</sup>

### Antimicrobial property of nanofiber membrane

Electrospun cellulose acetate nanofiber (CANF) and electrospun CHX loaded cellulose acetate nanofiber (CHX-CANF) were subjected to antimicrobial testing against *E. coli* and *S. aureus* using the disk-diffusion method following the United States Pharmacopeia 30 NF 25, 2007 <87> Biological Reactivity Tests *in vitro* test reference. For the test, 10 mm x 10 mm of electrospun cellulose acetate nanofiber (CANF) and electrospun CHX loaded cellulose acetate nanofiber (CHX-CANF) samples were used. 30 µg of amikacin and 1 µg oxacillin were used as positive control for *E. coli* and *S. aureus*, respectively, while a sample-free disc was used as negative control.

## RESULTS AND DISCUSSION

### Banana pseudostem fiber treatment

Banana pseudostem fibers were subjected to alkaline treatment or degumming in the presence of sodium hydroxide and sodium metabisulfite. Degumming was carried out to solubilize and remove the non-cellulosic components, such as gums (present as arabans and xylans), hemicelluloses, pectins and lignin present on the banana fibers, leaving behind the cellulose component of the fibers.<sup>23–26</sup>

### Chemical analysis of banana pseudostem fibers

Raw and treated banana fiber were subjected to fiber analyses to quantify the cellulose content and non-cellulosic component of fiber before and after the treatment. These were done to confirm the removal of the non-cellulosic components of the fiber after the treatment.

Based on the data (Table 1), there is a significant increase in the moisture content of treated banana fiber. This is due to the formation of pits and the removal of non-cellulosic components of fibers, especially of hydrophobic lignin, which facilitates the hydrophilicity of treated banana fibers.<sup>27,28</sup> Fiber analysis data also show the decrease in ethanol-benzene extractives and lignin for treated banana fibers. Ethanol-benzene extractives are non-cellulosic components of fiber, particularly, fats and waxes, which are usually found on the surface of the

fibers, and are commonly extracted with benzene.<sup>23</sup> These fats and waxes of banana fiber can also be removed by degumming, as they are readily soluble in an alkaline condition and thus are easy to remove, leading to a decrease in the ethanol-benzene extractives of alkaline treated banana fibers.<sup>29</sup> There is also a significant decrease in the lignin content of alkaline treated banana pseudostem fibers. This decrease in the lignin content of treated banana fibers is due to the solubilization and removal of lignin by the action of sodium hydroxide.<sup>24–26</sup> Under alkaline conditions, lignin from the fibers is removed by the reaction of hydroxide with the hydroxyl group of lignin, forming phenolate as intermediate and converting it to enol ether as a final product.<sup>24</sup>

Also, there is a significant increase in the total cellulose and alpha-cellulose in treated fibers. This indicates the successful removal of the non-cellulosic components, which yields fibers with high cellulose content. The fiber analyses verified that the double degumming process successfully removed non-cellulosic components of banana fibers and yielded dissolving pulp with high cellulose content.

### FT-IR spectroscopy analysis of banana pseudostem fibers

Raw banana fibers and treated banana fibers were analyzed by FT-IR to confirm the successful removal of the non-cellulosic components of the fiber. The FT-IR spectra of raw and treated banana fibers (Fig. 1c) show vibrational bands at 3300 cm<sup>-1</sup> (O-H stretching vibration), 2900 cm<sup>-1</sup> (C-H stretching vibration), 1100 cm<sup>-1</sup> (C-O-C glycosidic stretch), indicating the cellulose moiety of the fibers. However, it is observed that there is a decrease in the intensity of the bands at 1731 cm<sup>-1</sup> and 1541 cm<sup>-1</sup> (C=O stretching vibration), while the band at 1242 cm<sup>-1</sup> (C-O stretching vibration) disappeared in the IR spectrum of treated banana fibers. This decrease confirms the successful removal of lignin and hemicelluloses from the banana fibers.<sup>30–32</sup>

Table 1  
Chemical composition of raw and treated banana fibers

Sample	Moisture content (%)	Ethanol-benzene extractives (%)	Lignin (%)	Total cellulose (%)	Alpha-cellulose (%)
Raw banana fiber	7.12 (±0.14)	6.57 (±2.26)	15.16 (±0.91)	81.04 (±1.84)	63.97 (±2.12)
Treated banana fiber	7.71 (±0.25)	1.92 (±0.27)	4.43 (±1.48)	98.23 (±1.02)	94.61 (±0.70)

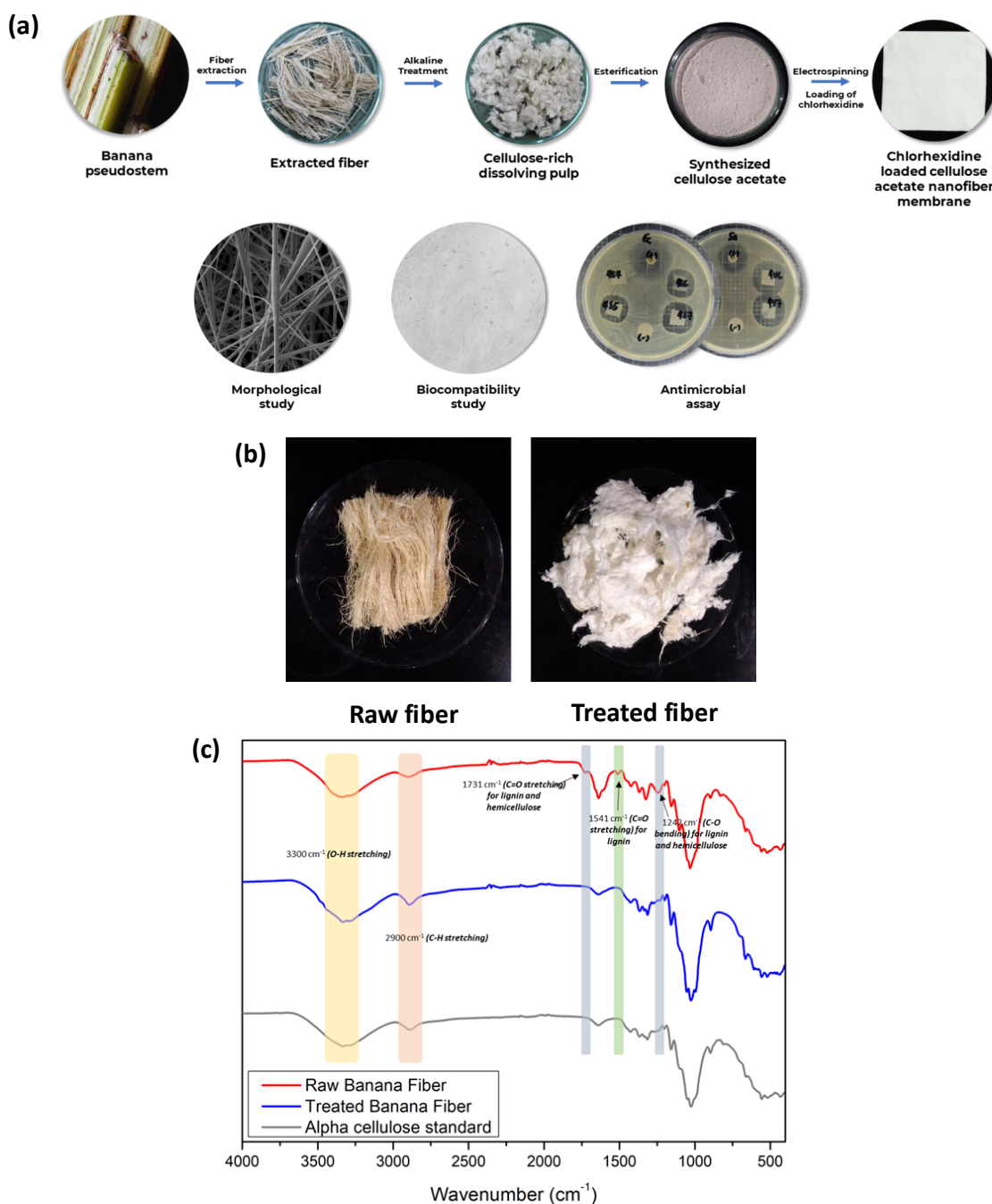


Figure 1: (a) Preparation of biocompatible and antimicrobial cellulose acetate nanofiber from banana pseudostem fibers, (b) raw and alkali treated banana pseudostem fibers and (c) FT-IR spectra of raw and alkali treated banana pseudostem fibers

Also, it can be remarked that the FT-IR spectral profile of the treated banana fiber is similar to that of the alpha-cellulose standard, which is indicative of the high cellulose content of treated banana fiber.

### Synthesis of cellulose acetate

Cellulose acetate was synthesized using the cellulose-rich dissolving pulp material derived from the alkaline-treated banana fibers through the esterification method, using acetic acid and acetic anhydride in the presence of acid catalyst.<sup>25,33</sup> The actual synthesis of cellulose

acetate from the alkaline treated banana fibers resulted in a white powder product (Fig. 2a).

### Degree of substitution of cellulose acetate

The degree of substitution of the synthesized cellulose acetate was determined using titrimetry.<sup>34</sup> The degree of substitution (DS) of cellulose acetate is the average number of acetyl groups per glucose unit. The value can be 0 for unsubstituted cellulose to 3 for cellulose triacetate.<sup>34</sup> Cellulose monoacetate has a degree of substitution from 0.5 to 1.1,<sup>35</sup> while cellulose diacetate is categorized as having a degree of substitution from 2.3 to 2.6, and cellulose triacetate has a degree of substitution from 2.8 to 3.<sup>36,37</sup> The determined % acetyl groups of synthesized cellulose acetate is 40.37 ( $\pm 0.67$ ), with the corresponding degree of substitution of 2.51 ( $\pm 0.07$ ).

Determining the degree of substitution of cellulose acetate is of utmost importance for the preparation of cellulose acetate, as the degree of substitution of acetate groups on cellulose affects the solubility, biodegradability and physical properties of the cellulose acetate.<sup>7,34,37,38</sup> In terms of solubility, cellulose diacetate is soluble in acetone, dioxane, methyl acetate and

tetrahydrofuran, while cellulose triacetate is soluble in dichloromethane and other chlorinated solvents.<sup>7,38,39</sup> Unsubstituted cellulose, on the other hand, is insoluble in many solvents.<sup>38,40</sup> In terms of biodegradability, cellulose acetate is more biodegradable when the degree of substitution is lower.<sup>34,41</sup> The DS value of 2.51 for the synthesized cellulose acetate from banana fiber confirms that the product is cellulose diacetate.

### FT-IR spectroscopy analysis of synthesized cellulose acetate

The FT-IR spectrum of the synthesized cellulose acetate (Fig. 2b) reveals a decrease in intensity of the O-H stretching vibration at 3300  $\text{cm}^{-1}$ , which indicates some O-H bonds participated in the formation of the ester bond with the acetate group. Also, the presence of strong intensity bands are observed at 1735  $\text{cm}^{-1}$  (C=O stretching vibration of acetate), 1371  $\text{cm}^{-1}$  (C-H bending vibration of acetate) and 1230  $\text{cm}^{-1}$  (C-O bending vibration of acetate), indicative of the presence of acetate groups in the synthesized products.<sup>25,33,41</sup> These observations confirm the successful conversion of banana fibers into cellulose acetate.

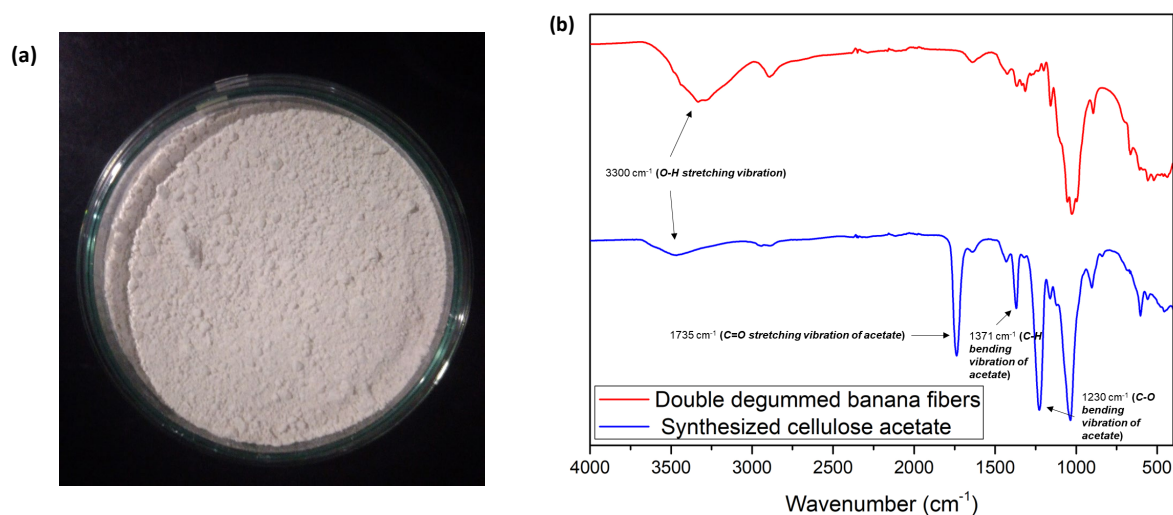


Figure 2: (a) Cellulose acetate synthesized from banana pseudostem fibers, and (b) FT-IR spectra of banana fibers and synthesized cellulose acetate

### Electrospun cellulose acetate nanofibers

The synthesized cellulose acetate powder derived from banana pseudostem fibers was converted into nanofiber (Fig. 3a) through electrospinning. Prior to the electrospinning process, cellulose acetate powder was dissolved in 2:1 acetone:*N,N*-dimethylacetamide binary

solvent, as this versatile solvent system provides continuous electrospinning of cellulose acetate into nanofibers.<sup>42</sup> Antimicrobial drug chlorhexidine was incorporated in the cellulose acetate. For the loading of chlorhexidine on nanofibers, chlorhexidine was dissolved in the cellulose acetate polymer solution and mixed to

evenly distribute the drug in the polymer solution. This approach of drug loading on nanofiber allows obtaining a drug loaded nanofiber membrane, in which the drug is embedded in the nanofiber matrix.<sup>43</sup>

### FT-IR spectroscopy analysis of electrospun cellulose acetate nanofibers

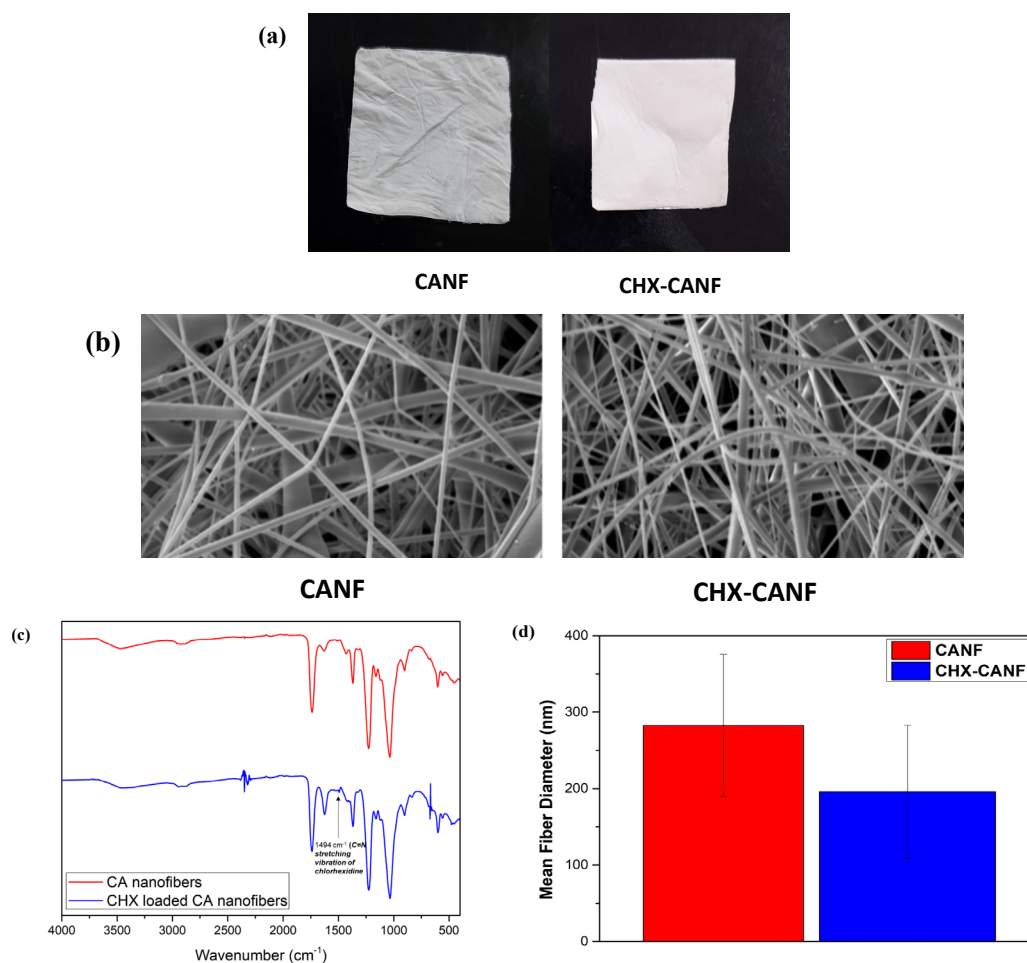
The electrospun nanofibers were subjected to FT-IR analysis to confirm the successful incorporation of the drug chlorhexidine in the nanofiber matrix.

As shown in the data (Fig. 3c), the FT-IR spectra of electrospun cellulose acetate nanofiber (CANF) and the electrospun chlorhexidine loaded cellulose acetate nanofiber (CHX-CANF) show the cellulose acetate identity of the nanofiber membrane, but there is a small peak occurring at  $1494\text{ cm}^{-1}$  in the spectrum of the drug loaded nanofiber membrane, which shows the C=N stretching vibration.<sup>44</sup> This indicates the presence of chlorhexidine in the nanofiber matrix and confirms the successful incorporation of

chlorhexidine in the cellulose acetate nanofiber membrane.

### Surface morphology and fiber diameter measurement of electrospun nanofibers

SEM imaging was used to investigate the surface morphology of the nanofiber membranes and to measure their fiber diameter. SEM images of cellulose acetate nanofiber (CANF) and chlorhexidine loaded cellulose acetate nanofiber (CHX-CANF) (Fig. 3b) show the typical fibrous morphology of nanofibers. The addition of chlorhexidine does not affect the overall morphology of the nanofibers. As presented in Figure 3d, CHX loaded nanofibers have the average fiber diameter of  $195.94 (\pm 86.83)$  nm, while the unloaded nanofibers have the average fiber diameter of  $282.72 (\pm 92.87)$  nm. Nanofibers with a diameter around 100-300 nm facilitate cell proliferation and viability, in contrast to nanofibers with larger fiber diameter ( $>1000$  nm).<sup>45,46</sup> Therefore, the fabricated nanofibers were expected to show good cell adhesion and proliferation for human cell lines.



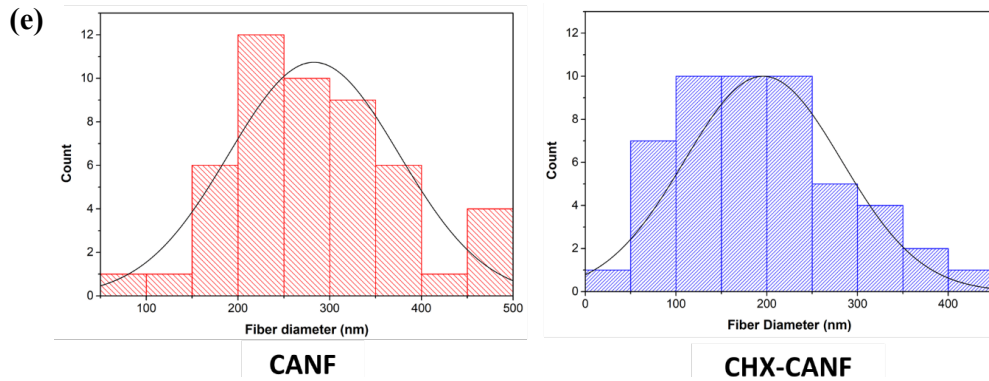


Figure 3: (a) Cellulose acetate nanofiber and CHX loaded cellulose acetate nanofiber, (b) SEM images of nanofibers, (c) FT-IR spectra of the nanofibers, (d) fiber diameter of the nanofibers and (e) fiber diameter distribution of nanofibers

Fiber diameter measurements of nanofibers (Fig. 3e) are normally distributed and it is observed that most of the fibers have the diameter of 200-300 nm. Overall, the CANF and CHX-CANF show smooth morphology, with uniform distribution of nanofibers and no beading. This smooth and uniform surface morphology of

nanofibers would greatly facilitate cell adhesion and proliferation.<sup>5</sup> In addition, the formation of beaded nanofiber is likewise avoided, being known that beaded nanofibers impede cell adhesion and proliferation.<sup>47</sup>

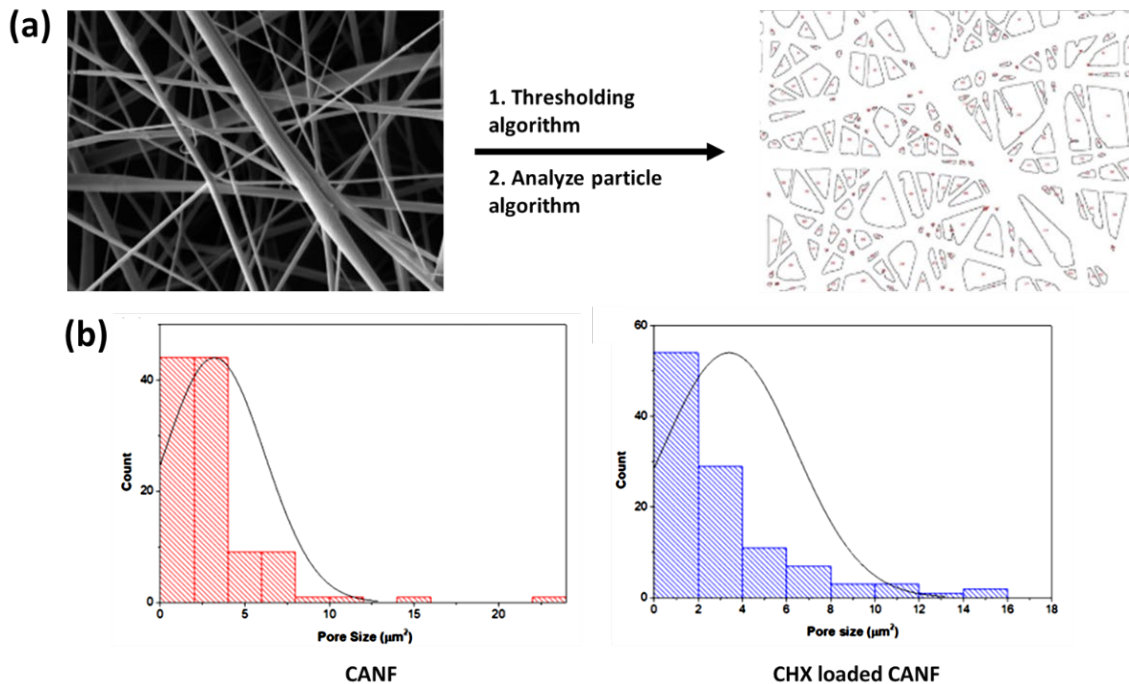


Figure 4: (a) Determination of porosity of nanofiber membranes through ImageJ and (b) pore size distribution of nanofibers

### Porosity measurement of electrospun nanofiber

Porosity measurements were done by image analysis using ImageJ software. The analysis involves the conversion of an SEM image into a binary image using the thresholding algorithm of the software. In the binary image, the porous section is represented by dark spots and its area is measured using the “Analyze particle” algorithm

of the software, yielding the pore size measurements and percent porosity of the material<sup>48</sup> (Fig. 4a).

Cellulose acetate nanofiber (CANF) has the estimated mean pore size of 3.40  $\mu\text{m}^2$  with the corresponding estimated percent porosity of 34.03%, while the chlorhexidine loaded cellulose acetate nanofiber has the estimated mean pore size of 3.20  $\mu\text{m}^2$ , with the corresponding

estimated percent porosity of 32.22% (Table 2). This indicates that the incorporation of chlorhexidine has no effect on the porosity of the nanofibers. The porosity of a nanofiber material is essential for wound healing and tissue engineering applications, as the pores present in the nanofiber matrix enhance the adhesion, migration and proliferation of cells, and facilitate the exchange of oxygen and nutrients in the tissue area.<sup>5</sup> It is observed that nanofibers that have larger pore size promote cell and tissue

proliferation.<sup>49</sup> The high porosity of the fabricated nanofiber makes it a good candidate as wound healing scaffold.

### Elemental analysis of electrospun nanofiber by energy dispersive X-ray spectroscopy

Alongside with SEM analysis, the nanofibers were subjected to EDX analysis to investigate the elements present in the material and to further confirm the successful incorporation of chlorhexidine into the nanofibers (Fig. 5).

Table 2  
Porosity of electrospun cellulose acetate nanofibers

Sample	Mean pore size ( $\mu\text{m}^2$ )	% Porosity
CANF	3.40 ( $\pm 3.01$ )	34.03
CHX-CANF	3.20 ( $\pm 2.98$ )	32.22

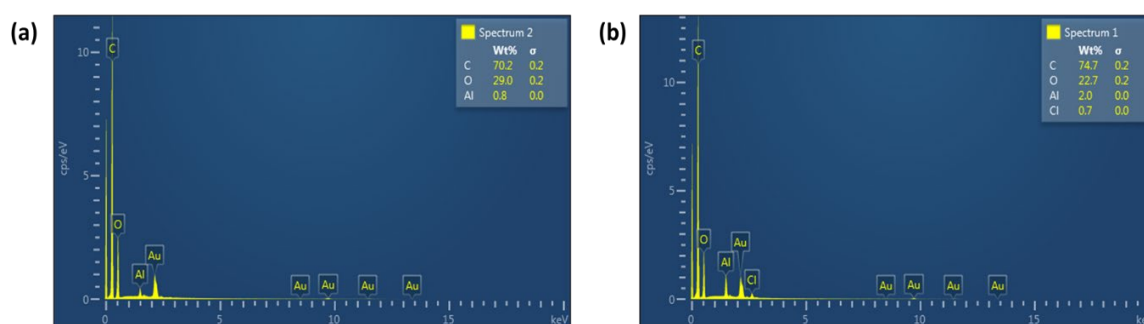


Figure 5: EDX spectra of (a) cellulose acetate nanofiber membrane and (b) chlorhexidine loaded cellulose acetate nanofiber membrane

The carbon percent in CANF and CHX-CANF was 70.77 ( $\pm 0.60$ ) and 69.9 ( $\pm 4.39$ ), respectively, while the oxygen percent in CANF and CHX-CANF was 28.67 ( $\pm 0.58$ ) and 23.7 ( $\pm 0.92$ ), respectively. The EDX spectra also revealed a significant amount of Cl present (0.7% Cl) in the chlorhexidine loaded cellulose acetate nanofibers and no trace of Cl present on the cellulose acetate nanofibers. This observation further confirms the successful incorporation of chlorhexidine into the nanofibers.

### Biocompatibility of electrospun nanofiber

The MTT cytotoxicity assay was employed to investigate the biocompatibility of drug loaded nanofibers. In the study, human intestinal epithelial cells (HIEC-6) were used. The MTT assay is primarily used to measure the cellular metabolic activity, to assess the cytotoxicity of a material or substance. The assay is colorimetric in nature<sup>50</sup> and based on the reduction of yellow tetrazolium salt (3-(4,5-dimethylthiazol-2-yl)-2,5-diphenyltetrazolium bromide or MTT) to purple

formazan crystals by live and metabolically active cells due to the presence of NADH/NADPH containing oxidoreductase in cells.<sup>51–53</sup> The insoluble formazan crystals are further dissolved by the solubilizing agent (*e.g.*, DMSO) and the resulting solution is measured using a UV-Vis spectrophotometer. The darker the solution, the greater the number of viable cells in a solution.

In the photomicrograph (Fig. 6a), the presence of viable HIEC-6 cells is observed after incubation with chlorhexidine loaded nanofiber membranes compared to the positive control. The proliferation of viable HIEC-6 cells in chlorhexidine loaded cellulose acetate nanofiber membranes indicates low cytotoxicity of the nanofiber membrane and shows good biocompatibility with mammalian cells. This observation is further confirmed by the percent cell inhibition data of the nanofiber membrane (Fig. 6b). It is observed that increasing the chlorhexidine loading on nanofibers increases the percent cell inhibition (percent inhibition ranging from 2.47% to 14.57%), however it is much lower

than that of the mitomycin C positive control (percent inhibition of 38.51%). The relatively low percent cell inhibition of chlorhexidine loaded nanofibers, compared to mitomycin C, indicates the low cytotoxic nature of the nanofibers.

In addition to the percent cell inhibition, half maximal inhibitory concentration ( $IC_{50}$ ) was determined from the assay.  $IC_{50}$  is a quantitative measurement of how much of a substance is needed to inhibit the biological component (*e.g.* enzyme, cell and microorganism) by 50%.<sup>54</sup> It is a measurement of potency of any substance to inhibit biological and biochemical processes and function. The  $IC_{50}$  of chlorhexidine loaded cellulose acetate nanofiber membrane (from 0.5% to 1.5% CHX) is greater than 100  $\mu\text{g/mL}$ , compared to the  $IC_{50}$  of 1.99  $\mu\text{g/mL}$  for the mitomycin C positive control. Any substance that has an  $IC_{50}$  of less than 30  $\mu\text{g/mL}$  is said to have

potent cytotoxic activity.<sup>22</sup> The high  $IC_{50}$  of the nanofibers shows the low potency of the nanofibers to inhibit the biological processes of cells and indicates good biocompatibility with the cells.

### Antimicrobial property of electrospun nanofiber

Electrospun cellulose acetate nanofiber (CANF) and electrospun chlorhexidine loaded cellulose acetate nanofiber (CHX-CANF) were subjected to antimicrobial assays against *E. coli* and *S. aureus*, following the disk diffusion method (Fig. 7). The antimicrobial activity of chlorhexidine (CHX) is due to the capability of the chlorophenyl guanide group of CHX to penetrate through the cell wall of the bacteria, then irreversibly disrupting bacterial membrane, thus killing the microbes.<sup>44</sup>

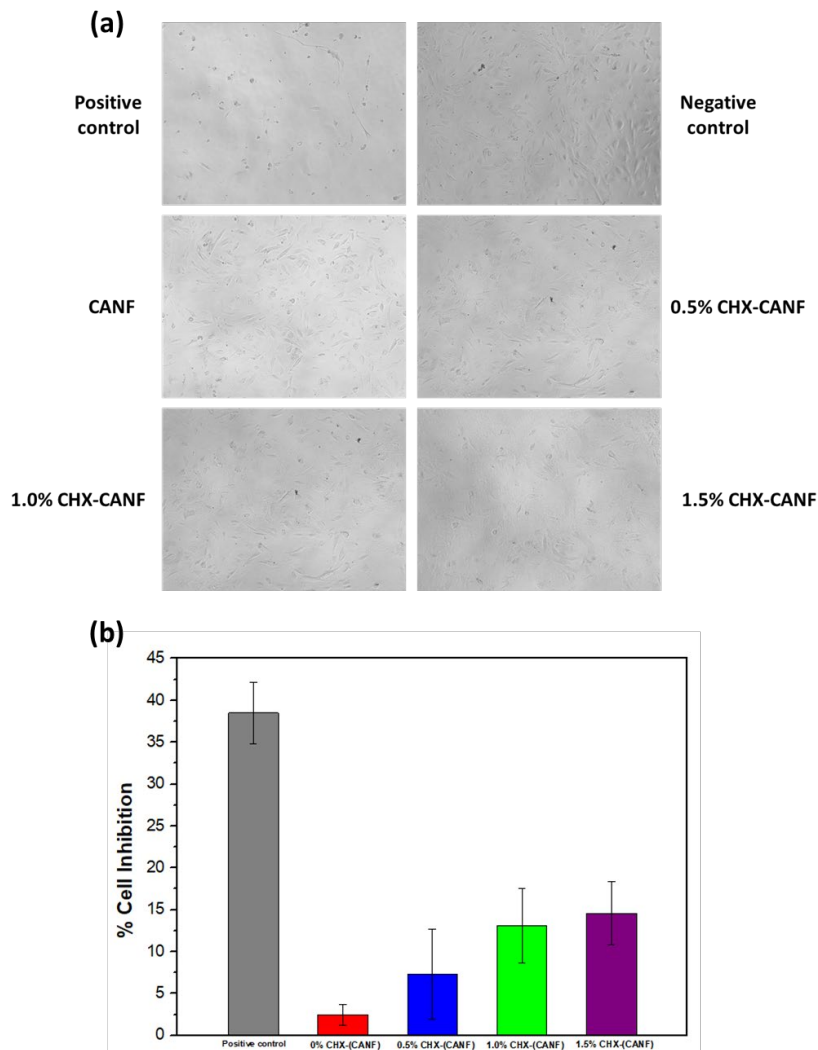


Figure 6: (a) Photomicrographs of HIEC-6 cells incubated with nanofiber membrane, and (b) % cell inhibition of HIEC-6 in cellulose acetate nanofiber membrane loaded with different concentration of chlorhexidine

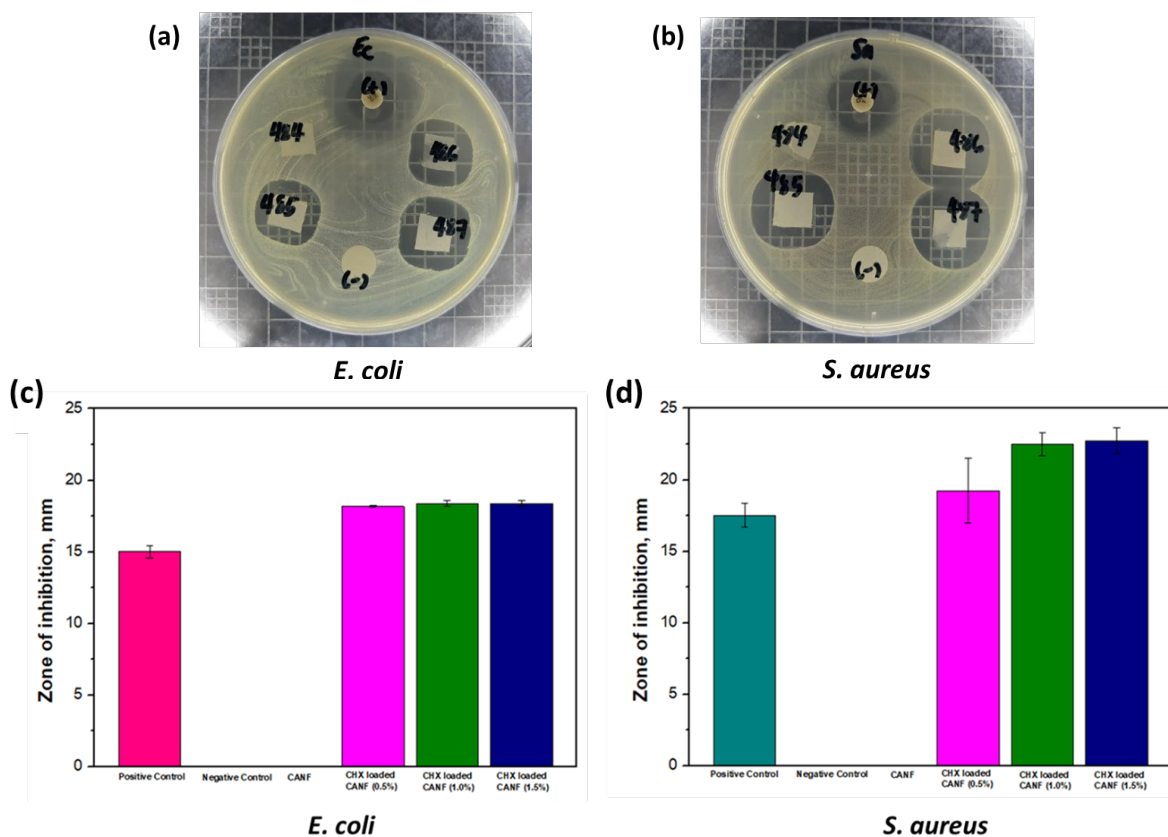


Figure 7: Antimicrobial assay of CHX-CANF against (a) *E. coli* and (b) *S. aureus*, and zone of inhibition of CHX-CANF on (c) *E. coli* and (d) *S. aureus*

Table 3  
Inhibitory activity and reactivity of drug loaded nanofiber membrane against *E. coli* and *S. aureus*

Sample	<i>E. coli</i>		<i>S. aureus</i>	
	Inhibitory activity	Reactivity	Inhibitory activity	Reactivity
Positive control	+++	3	+++	4
Negative control	-	0	-	0
CANF	-	0	-	0
CHX loaded CANF (0.5%)	+++	3	+++	3
CHX loaded CANF (1.0%)	+++	3	+++	4
CHX loaded CANF (1.5%)	+++	4	+++	4

Inhibitory activity rating: (+++) complete; (++) partial; (+) slight; (-) negative

Reactivity rating: 0 – None (no detectable zone around or under specimen), 1 – Slight (some malformed or degenerate cells under the specimen), 2 – Mild (zone limited under the specimen), 3 – Moderate (zone extended 5 to 10 mm beyond the specimen), 4 – Severe (zone extended more than 10 mm beyond the specimen)

CHX-CANF exhibited complete inhibitory activity and moderate to severe reactivity against *E. coli*, compared to the nanofiber membrane with no CHX. This indicated the potent antimicrobial activity of CHX fixed on the nanofiber matrix. This observation is supported by the large zone of inhibition (ZOI) of the nanofiber membrane against *E. coli*. Similarly, the chlorhexidine loaded nanofiber membrane also exhibited complete inhibitory activity and severe reactivity

against *S. aureus*, associated with a large zone of inhibition. These observations confirm the good antimicrobial activity of chlorhexidine loaded nanofiber membrane (Fig. 7c, 7d and Table 3).

As regards the chlorhexidine loading in the nanofibers, 1.0% w/v CHX serves as the optimum amount, as this CHX amount gives potent antimicrobial property (ZOI: *E. coli* – 18.38 mm and *S. aureus* – 22.51 mm), while achieving low cytotoxicity (percent cell inhibition: 13.07% and

IC<sub>50</sub>: >100 µg/mL) with human intestinal epithelial cell line HIEC-6.

## CONCLUSION

A biocompatible and antimicrobial nanofiber material was successfully prepared from banana pseudostem fiber waste. The study was able to demonstrate the feasible conversion of banana pseudostem fiber into cellulose acetate nanofibers through alkaline treatment of fibers into cellulose-rich dissolving pulp, followed by esterification of the dissolving pulp into cellulose acetate and finally electrospinning of drug loaded cellulose acetate nanofibers. The nanofiber material shows excellent antimicrobial activity against Gram-positive and Gram-negative bacteria, and good biocompatibility with the human normal cell lines, making it a good candidate biomaterial to be used as wound healing and tissue engineering scaffold. The successful preparation of this nanofiber membrane paves the way for the production of biomaterials for wound healing and tissue engineering applications from agricultural wastes and by-products, in a sustainable and environmentally friendly way.

## REFERENCES

- H. T. Lu, G.-Y. Huang, W.-J. Chang, T.-W. Lu, T. W. Huang *et al.*, *Carbohydr. Polym.*, **281**, 119035 (2022), <https://doi.org/10.1016/j.carbpol.2021.119035>
- H. R. Amaral, J. A. Wilson, R. J. F. C. do Amaral, I. Paço, F. C. S. de Oliveira *et al.*, *Carbohydr. Polym.*, **252**, 117201 (2021), <https://doi.org/10.1016/j.carbpol.2020.117201>
- J. Shen, R. Chang, L. Chang, Y. Wang, K. Deng *et al.*, *Carbohydr. Polym.*, **281**, 119052 (2022), <https://doi.org/10.1016/j.carbpol.2021.119052>
- Q. Zhang, H. Lu, N. Kawazoe and G. Chen, *J. Bioact. Compat. Polym.*, **28**, 426 (2013), <https://doi.org/10.1177/0883911513494620>
- G. Ramanathan, L. S. S. Sobhanadhas, G. F. Sekar Jeyakumar, V. Devi, U. Tiruchirapalli Sivagnanam *et al.*, *Biomacromolecules*, **21**, 2512 (2020), <https://doi.org/10.1021/acs.biomac.0c00516>
- D. Atila and D. Keskin, *Carbohydr. Polym.*, **133**, 251 (2015), <https://doi.org/10.1016/j.carbpol.2015.06.109>
- B. Volkert and W. Wagenknecht, *Macromol. Symp.*, **262**, 89 (2008), <https://doi.org/10.1002/masy.200850211>
- R. Konwarh, N. Karak and M. Misra, *Biotechnol. Adv.*, **31**, 421 (2013), <https://doi.org/10.1016/j.biotechadv.2013.01.002>
- H. Liu and C. Tang, *Polym. J.*, **39**, 65 (2007), <https://doi.org/10.1295/polymj.PJ2006117>
- S. Ok, J. Ho, K. Dan, Y. Ok and W. Ho, *Mater. Lett.*, **62**, 759 (2008), <https://doi.org/10.1016/j.matlet.2007.06.059>
- S. Tungprapa, T. Puangpam and M. Weerasombut, *Cellulose*, **14**, 563 (2007), <https://doi.org/10.1007/s10570-007-9113-4>
- W. Cui, Y. Zhou and J. Chang, *Sci. Technol. Adv. Mater.*, **11**, 014108 (2010), <https://doi.org/10.1088/1468-6996/11/1/014108>
- W. Li, X. Liu and X. He, *Carbohydr. Polym.*, **15**, 153 (2017), <https://doi.org/10.1016/j.carbpol.2016.12.013>
- B. S. Padam, H. S. Tin, F. Y. Chye and M. I. Abdullah, *J. Food Sci. Technol.*, **51**, 3527 (2012), <https://doi.org/10.1007/s13197-012-0861-2>
- D. Mohapatra, S. Mishra and N. Sutar, *Agric. Rev.*, **31**, 56 (2010)
- K. Getha and S. Vikineswary, *J. Ind. Microbiol. Biotechnol.*, **28**, 303 (2002), <https://doi.org/10.1038/sj/jim/7000247>
- S. K. Paramavisam, D. Panneerselvam, D. Sundaram, K. N. Shiva and U. Subbaraya, *J. Nat. Fibers*, **19**, 1333 (2022), <https://doi.org/10.1080/15440478.2020.1764456>
- Z. A. Ara, *J. Nat. Fibers*, **19**, 6469 (2021)
- M. S. Merai, N. Khairuddin, M. H. Salehudin and B. M. Siddique, *Membranes (Basel)*, **12**, 451 (2022), <https://doi.org/10.3390/membranes12050451>
- A. Alemdar and M. Sain, *Bioresour. Technol.*, **99**, 1664 (2008), <http://dx.doi.org/10.1016/j.biortech.2007.04.029>
- B. Soni, E. Barbary and B. Mahmoud, *Carbohydr. Polym.*, **134**, 581 (2015), <https://doi.org/10.1016/j.carbpol.2015.08.031>
- M. Jokhadze, L. Eristavi, J. Kutchukhidze, A. Chariot, L. Angenot *et al.*, *Phytother. Res.*, **21**, 622 (2007), <https://doi.org/10.1002/ptr.2130>
- Subagyo, A. & Chafidz, A., *InTechOpen*, 1–19 (2018).
- P. Lyu, Y. Zhang, X. Wang and C. Hurren, *Ind. Crop. Prod.*, **174**, 114158 (2021), <https://doi.org/10.1016/j.indcrop.2021.114158>
- A. M. Das, A. A. Ali and M. P. Hazarika, *Carbohydr. Polym.*, **112**, 342 (2014), <https://doi.org/10.1016/j.carbpol.2014.06.006>
- D. Tristantini and C. Sandra, *E3S Web Conf.*, *The 3<sup>rd</sup> International Tropical Renewable Energy Conference “Sustainable Development of Tropical Renewable Energy” (i-TREC 2018)*, vol. 67, 04035 (2018), <https://doi.org/10.1051/e3sconf/20186704035>
- M. Rashid, S. Samad, M. Gafur and A. M. Choudhury, *Int. J. Sci. Eng. Res.*, **6**, 1870 (2015)
- S. K. Paramasivam, D. Panneerselvam and D. Sundaram, *J. Nat. Fibers*, **19**, 4485 (2022), <https://doi.org/10.1080/15440478.2020.1863295>
- W. Li, Y. Zhang, J. Li, Y. Zhou, R. Li *et al.*, *Carbohydr. Polym.*, **132**, 513 (2015), <https://doi.org/10.1016/j.carbpol.2015.06.066>
- M. Jannah, M. Mariatti, A. Abu Bakar and H. P. Abdul Khalil, *J. Reinf. Plast. Compos.*, **28**, 1519

- (2009), <https://doi.org/10.1177/0731684408090366>
- <sup>31</sup> A. P. Bispo Gonçalves, C. S. De Miranda, J. C. De Oliveira, A. Moreira, F. Cruz *et al.*, *Mater. Res.*, **18**, 205 (2015), <https://doi.org/10.1590/1516-1439.366414>
- <sup>32</sup> A. Parre, B. Karthikeyan, A. Balaji and R. Udhayasankar, *Mater. Today Proc.*, **22**, 347 (2020), <https://doi.org/10.1016/j.matpr.2019.06.655>
- <sup>33</sup> G. R. Filho, D. Monteiro, C. da S. Meireles and R. M. N. de Assuncao, *Carbohydr. Polym.*, **73**, 74 (2008), <https://doi.org/10.1016/j.carbpol.2007.11.010>
- <sup>34</sup> E. Samios, R. K. Dart and J. V. Dawkins, *Polymer (Guildf)*, **38**, 3045 (1997), [https://doi.org/10.1016/S0032-3861\(96\)00868-3](https://doi.org/10.1016/S0032-3861(96)00868-3)
- <sup>35</sup> C. M. Buchanan, D. Dorschel, R. M. Gardner, R. J. Komarek, A. J. Matosky *et al.*, *J. Environ. Polym. Degrad.*, **4**, 179 (1996), <https://doi.org/10.1007/BF02067452>
- <sup>36</sup> R. H. Atalla and A. Isogai, in “Comprehensive Natural Products II: Chemistry and Biology”, edited by L. Mander and H.-W. Lui, Oxford, Elsevier, 2010, pp. 493–536
- <sup>37</sup> P. Fei, L. Liao and B. Cheng, *Anal. Methods*, **9**, 6194 (2017), <https://doi.org/10.1039/C7AY02165H>
- <sup>38</sup> R. R. M. De Freitas, A. M. Senna and V. R. Botaro, *Ind. Crop. Prod.*, **109**, 452 (2017), <https://doi.org/10.1016/j.indcrop.2017.08.062>
- <sup>39</sup> H. O. Ghareeb, F. Malz, P. Kilz and W. Radke, *Carbohydr. Polym.*, **88**, 96 (2012), <https://doi.org/10.1016/j.carbpol.2011.11.071>
- <sup>40</sup> H. Kono, H. Hashimoto and Y. Shimizu, *Carbohydr. Polym.*, **118**, 91 (2015), <https://doi.org/10.1016/j.carbpol.2015.04.009>
- <sup>41</sup> F. Z. Beraich, M. Bakasse and M. Arouch, in *Procs. 2016 International Renewable and Sustainable Energy Conference (IRSEC) 2016*, pp. 1–5
- <sup>42</sup> B. Tarus, N. Fadel, A. Al-Oufy and M. El-Messiry, *Alexandria Eng. J.*, **55**, 2975 (2016), <https://doi.org/10.1016/j.aej.2016.04.025>
- <sup>43</sup> E. J. Torres-Martinez, J. M. C. Bravo, A. S. Medina and G. L. P. Gonzalez, *Curr. Drug Deliv.*, **15**, 1360 (2018), <https://doi.org/10.2174/1567201815666180723114326>
- <sup>44</sup> L. Chen, L. Bromberg, T. A. Hatton and G. C. Rutledge, *Polymer (Guildf)*, **49**, 1266 (2008), <https://doi.org/10.1016/j.polymer.2008.01.003>
- <sup>45</sup> T. Hodgkinson, X. Yuan and A. Bayat, *J. Tissue Eng.*, **5**, 1 (2014), <https://doi.org/10.1177/20417314145516>
- <sup>46</sup> S. E. Noriega, G. I. Hasanova, M. Jeong, G. F. Larsen and A. Subramanian, *Cell Tissues Organs*, **68516**, 207 (2012), <https://doi.org/10.1159/000325144>
- <sup>47</sup> M. Chen, P. K. Patra, S. B. Warner and B. Sankha, *Tissue Eng.*, **13**, 579 (2007), <https://doi.org/10.1089/ten.2006.0205>
- <sup>48</sup> F. Zhou, G. J. M. Parker, S. J. Eichhorn and P. L. Hubbard, *Mater. Charact.*, **109**, 25 (2015), <https://doi.org/10.1016/j.matchar.2015.09.010>
- <sup>49</sup> J. Wu and Y. Hong, *Bioact. Mater.*, **1**, 56 (2016), <https://doi.org/10.1016/j.bioactmat.2016.07.001>
- <sup>50</sup> T. Mosmann, *J. Immunol. Methods*, **65**, 55 (1983), [https://doi.org/10.1016/0022-1759\(83\)90303-4](https://doi.org/10.1016/0022-1759(83)90303-4)
- <sup>51</sup> D. T. Vistica, P. Skehan, D. Scudiero, A. Monks, A. Pittman *et al.*, *Cancer Res.*, **51**, 2515 (1991)
- <sup>52</sup> T. F. Slater, B. Sawyer and U. Strauli, *Biochim. Biophys. Acta*, **77**, 383 (1963), [https://doi.org/10.1016/0006-3002\(63\)90513-4](https://doi.org/10.1016/0006-3002(63)90513-4)
- <sup>53</sup> M. V. Berridges and A. S. Tan, *Arch. Biochem. Biophys.*, **303**, 474 (1993), <https://doi.org/10.1006/abbi.1993.1311>
- <sup>54</sup> Y.-C. Cheng, and W. H., Prusoff, *Biochem. Pharmacol.*, **22**, 3099 (1973), [https://doi.org/10.1016/0006-2952\(73\)90196-2](https://doi.org/10.1016/0006-2952(73)90196-2)